NASA/TM—20230014257

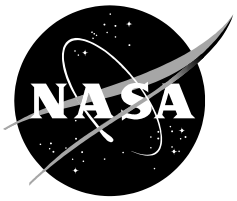

Evaluation of Elements used for Manufacturing of NanoLam Metallized Polymer Film Capacitors

Alexander A. Teverovsky

November 2023

NASA STI Program Report Series

The NASA STI Program collects, organizes, provides for archiving, and disseminates NASA's STI. The NASA STI program provides access to the NTRS Registered and its public interface, the NASA Technical Reports Server, thus providing one of the largest collections of aeronautical and space science STI in the world. Results are published in both non-NASA channels and by NASA in the NASA STI Report Series, which includes the following report types:

- TECHNICAL PUBLICATION. Reports of completed research or a major significant phase of research that present the results of NASA Programs and include extensive data or theoretical analysis. Includes compilations of significant scientific and technical data and information deemed to be of continuing reference value. NASA counterpart of peer-reviewed formal professional papers but has less stringent limitations on manuscript length and extent of graphic presentations.

- TECHNICAL MEMORANDUM. Scientific and technical findings that are preliminary or of specialized interest, e.g., quick release reports, working papers, and bibliographies that contain minimal annotation. Does not contain extensive analysis.

- CONTRACTOR REPORT. Scientific and technical findings by NASA-sponsored contractors and grantees.

- CONFERENCE PUBLICATION. Collected papers from scientific and technical conferences, symposia, seminars, or other meetings sponsored or co-sponsored by NASA.

- SPECIAL PUBLICATION. Scientific, technical, or historical information from NASA programs, projects, and missions, often concerned with subjects having substantial public interest.

- TECHNICAL TRANSLATION. English-language translations of foreign scientific and technical material pertinent to NASA's mission.

Specialized services also include organizing and publishing research results, distributing specialized research announcements and feeds, providing information desk and personal search support, and enabling data exchange services.

For more information about the NASA STI program, see the following:

- Access the NASA STI program home page at http://www.sti.nasa.gov

- Help desk contact information:

https://www.sti.nasa.gov/sti-contact-form/ and select the "General" help request type.

NASA/TM—20230014257

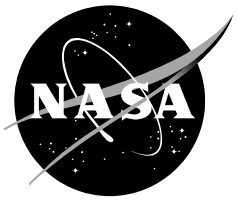

Evaluation of Elements used for Manufacturing of NanoLam Metallized Polymer Film Capacitors

Alexander A. Teverovsky
Jacobs Engineering Group, Lanham MD

National Aeronautics and
Space Administration

Goddard Space Flight Center
Greenbelt, MD 20771

November 2023

Acknowledgments (optional)

This work was sponsored by the NASA Electronic Parts and Packaging (NEPP) Program.

Available from

NASA STI Program
Mail Stop 148
NASA's Langley Research Center
Hampton, VA 23681-2199

National Technical Information Service
5285 Port Royal Road
Springfield, VA 22161
703-605-6000

This report is available in electronic form at

https://nepp.nasa.gov/

Evaluation of Elements used for Manufacturing of NanoLam Metallized Polymer Film Capacitors

Abstract

Metallized polymer film capacitors (MPFC) manufactured by NanoLam technology have a better volumetric efficiency and performance that may exceed the reliability of conventional MPFCs typically used in power and high voltage systems that require high insulation resistance and low power losses. These capacitors can be also an effective replacement for electrolytic and stacked ceramic capacitors currently used in space applications looking to save significant volume and mass. This report evaluates the effects of environmental conditions including radiation and storage at room and high temperatures on the characteristics of NanoLam elements used in the production of MPFCs. Assessments of the reliability acceleration factors and predictions for the useful life are made based on highly accelerated life tests (HALT) using distributions of times to parametric failures at different stress conditions. It has been shown that even a relatively small amount of moisture absorbed at room environments in the dielectric layers may substantially change the probability of failure. In the presence of moisture, degradation processes that started after voltage application continue with time during storage.

Contents

I. Introduction

Manufacturing of NanoLam capacitors can be presented as a two-step process. The first step is the formation of NanoLam Elements (NLE) for capacitors, and the second is stacking of the elements, attaching leads and encapsulation in plastic packages. Examples of an assembled capacitor, case and NLEs are shown in Fig.I.1.

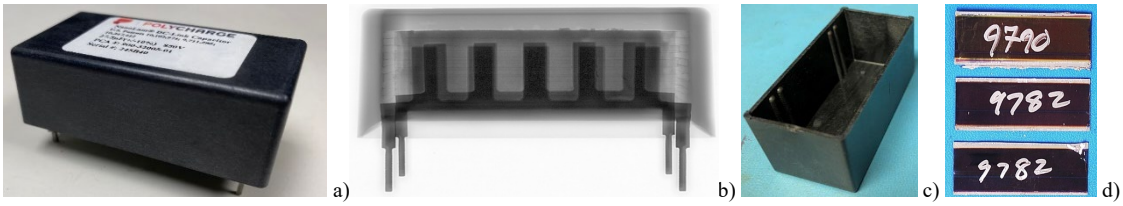

a) b) c) d)

Fig. I.1. An external (a) and side X-ray (b) views of an assembled NanoLam capacitor, an overall view of the case (c), and 200 μF 50 V elements used for stacking (d).

NLEs are formed in a vacuum process that includes vapor deposition of thin (few hundreds of nanometers) polymer films by electron-beam curing of acrylate-based monomers followed by a deposition of Al metallization with a thickness of dozens of nanometers. The formed polymer has dielectric constant in the range from 2.6 to 9 [1, 2] that exceeds dielectric constant of polypropylene (PP) that is typically used in conventional MPFCs ($\varepsilon = 2.2$). Multiple deposition cycles result in the formation of sheets with thousands of metallized polymer layers that are then cut into relatively small cards. Polymer at the contact areas is removed by plasma ashing (scooping) to allow contact with metallization at terminals, which are formed by the arc spraying of zinc, resulting in terminations similar to the ones used for standard MPFCs. NanoLam technology replaces a three-step process in conventional MPFCs that includes polymer extrusion, metallization and winding with a one step process in a vacuum chamber. Formation of vacuum tight polymer-metallization interfaces reduces the probability of partial discharge. Also, the presence of oxygen in the molecular structure of the polymer allows for oxidation of aluminum metallization and enhances the efficiency of self-healing in case a local breakdown in the dielectric.

Before assembly, the elements are tested to screen-out defects by a short burn-in (20 hours at 140 ºC and 66 V) and measured for their capacitance, dissipation factor (DF), equivalent series resistance (ESR), and leakage currents. Before encapsulation, the stacked elements are baked out at 125 ºC for 15-20 hours. Engineering samples of the new technology capacitors are currently manufactured by PolyCharge America, Inc. (PCA). Rubicon is manufacturing low voltage general purpose PMLCAPs based on NanoLam technology from 2009. Exxelia had begun commercial production of Miniature Micro-Layer TM (MML®) capacitors using NanoLam technology elements licensed by PCA in 2022 [3]. The parts have higher than standard MPFCs energy density and can operate reliably up to 140 ºC.

Quality and reliability of the assembled NanoLam capacitors depend on characteristics and performance of NLEs to a great degree. Degradation with time over operation of all types of MPFC, NLE included, is due to self-healing processes that cause a gradual decrease of capacitance and an increase of DF and ESR [4-6]. Analysis of the variations of AC characteristics in MFPCs is often used for reliability assessments and development of predictive models to assess the probability of parametric failures.

In this work, characteristics and behavior of NLEs rated to 50 V have been analyzed at different environmental conditions including high temperature storage (HTS), and gamma radiation. Effects of moisture on the rate of degradation have been studied by testing samples over time at room conditions with and without pre-bake. Voltage and temperature reliability acceleration factors were assessed by highly accelerated life testing (HALT) using a general Weibull log-linear model at voltages from 75 to 150 V and temperatures from 20 to 145 ºC. The efficiency of self-healing was assessed by monitoring leakage currents during HALT.

II. Experiment

Four lots of 200 μF and one lot of 45 μF NLEs, all rated to 50 V, were employed for this study. One lot of 200 μF and 45 μF elements were manufactured in 2022 (lot 2022). Three other lots of 200 μF elements were manufactured in 2023 (lot 68, lot 73, and lot 76). All 200 μF elements have a size 54.6×21.2×1 mm and mass of 1.4 g; 45 μF capacitors have a size of 25.4×12.1×1 mm and mass of 0.35 g. All lots were produced using the same processes and materials and were comprised of 2000 metallized polymer layers with a thickness of ~0.25 μm.

Capacitance and DF of the parts were measured at 120 Hz, and ESR at 100 kHz. Leakage currents were monitored over time at the rated voltage to determine DCL, and during stress testing to assess the efficiency of self-healing. The currents were monitored using a PC based system that included a power supply, scanner, and voltmeter that measured voltages across the current sense resistors connected to each capacitor.

An example of degradation of AC characteristics of stacked 50 V NLEs forming a 750 µF capacitor at room temperature and 100 V for 2500 hours is shown in Fig. II.1. Variations of all characteristics can be accurately approximated with lines that allow for calculations of the relevant degradation rates. However, results displayed in Fig.II.1 as well as other tests in this study show that the spread of data for DF and ESR is greater than for capacitance measurements. For this reason, the degradation rate was estimated based on capacitance variations.

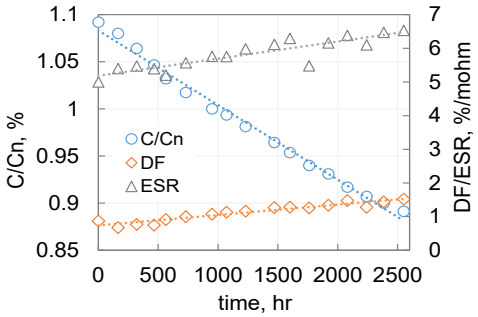

Fig. II.1. Degradation of normalized capacitance, dissipation factor and ESR for a 750 µF 50 V capacitor tested at 20 ºC and 100 V.

Typical relaxation of polarization and depolarization currents in NLEs is shown in Fig.II.2. Similar to other types of capacitors, the relaxation follows Curie–von Schweidler law, $I(t) = I_0 \times t^{-m}$, where I_0 and m are constants. The exponent m typically has values close to 1. Results in Fig.II.2 indicate that measurements of insulation resistance that are carried out within 2 min of electrification reflect absorption rather than intrinsic conductivity processes in the dielectric. The intrinsic leakage currents are below 10 nA, and the relevant IR values exceed 5 Gohm. Absorption capacitance, C_t, was calculated as a ratio of the charge transferred during depolarization, Q_t, and test voltage during polarization, $C_t = Q_t/V_{test}$. The values of Q_t were estimated based on depolarization currents by integration from 1 to 10,000 sec:

$$Q_t = \frac{I_0}{1-m} \times t^{1-m}\Big|_1^{1000} \qquad \text{(II.1)}$$

The transferred charge increases linearly with voltage up to 1.6VR (Fig. II.2.b) that allows characterization of the process by absorption capacitance, C_t. Estimations showed that NLEs have C_t ~3% of the nominal capacitance value. This is substantially less than for X7R ceramic capacitors (~25%) [7] and for tantalum capacitors (~ 12%) [8] and corresponds to a much lower polymer dielectric absorption and respectively to lower absorption voltages in MPFCs [5]. These data correspond to approximately tenfold reduction of dielectric absorption in NanoLam capacitors compared to X7R capacitors [9].

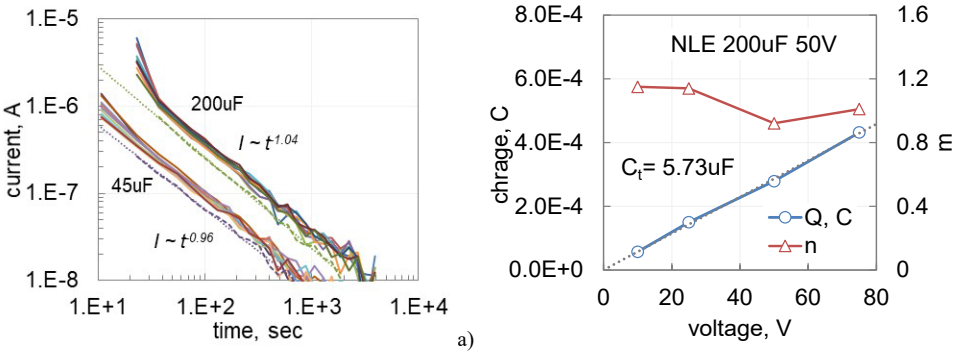

Fig. II.2. Relaxation of polarization (solid lines) and depolarization (dashed lines) currents in NL elements at 50 V and 20 ºC (a) and voltage dependence of the transferred charge, Q_t, and exponent m (b).

III. Effect of gamma radiation

Five elements of 200 µF 50 V capacitors from lot 76 have been tested over time with exposure to Co-60 irradiation at a rate of 39 rad per sec. Capacitance, DF, ESR, DCL and absorption capacitance, C_t was measured initially and then periodically up to 5 Mrad (Si) of total ionizing doze (TID). Results of these measurements are shown in Fig.III.1 and Fig. III.2 and indicate a relatively minor degradation of electrical characteristics. On average, capacitance increased by 5 ±0.25%, DF by 38 ±25%, and ESR by 93 ±60%. Polarization leakage currents decreased almost an order of magnitude and absorption currents increased 2 - 2.5 times. The absorption capacitance decreased by 2 to 3% and the exponent *m* was in the range from 1.1 to 1.15. A high radiation tolerance of other types of MPFCs was reported before. For example, polypropylene films and capacitors remained operational up to 100 Mrad [10, 11].

It is known that gamma radiation can induce growth of the aluminum hydroxide layers and increase resistance of thin aluminum films [12]. For NLEs, this would cause an increase to ESR, and as a result, decrease of capacitance. Data show that this type of degradation up to 5 Mrad Si is not substantial and does not change characteristics of the capacitors significantly.

Before irradiation, the parts were stored at room conditions (RC) for a few days. Each irradiation cycle took less than 7 hours, and the measurements were taken within an hour. Before each radiation step, the parts were kept at room conditions, so the total time of the testing spanned 3 months. It is possible, that a substantial portion of capacitance increase was attributed not to the radiation effect but to additional moisture absorption in the process of storage at RC. Measurements showed that temperature and humidity at RC were 21.5 ±0.4 ºC and 50 ±2% RH.

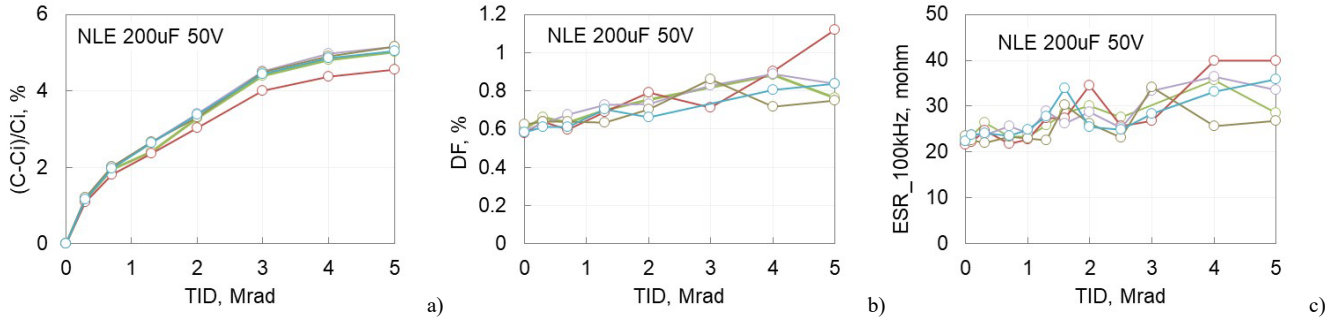

Fig. III.1. Variations of the normalized values of capacitance variations (a), DF (b), and ESR (c) for five samples of lot 76 NLEs during gamma radiation testing.

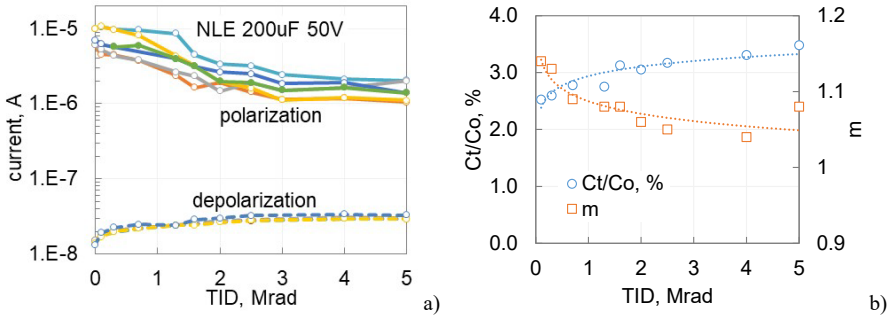

Fig. III.2. Effect of radiation on leakage currents measured after 1000 sec of polarization and depolarization (a) and on normalized values of absorption capacitance and the exponent *m* (b).

To verify the effect of storage, measurements of capacitance continued over time of storage, first during 400 hours at RC, then during 180 hours of annealing at 100 ºC, and finally again at RC for 1000 hours. A reduction of capacitance by ~6% after bake and the following recovery during storage at RC is shown in Fig. III.3.a. The increase of capacitance after annealing at 100 ºC exceeded 4%, so possible degradation caused by 5 Mrad TID was below 2%. The values of ESR did not change significantly during post-radiation tests (Fig. III.3.b). The results confirmed that the observed changes were mostly due to moisture absorption in the process of storage between irradiation cycles. Analysis of the effect of moisture on characteristics of the parts is given in the next section of the report.

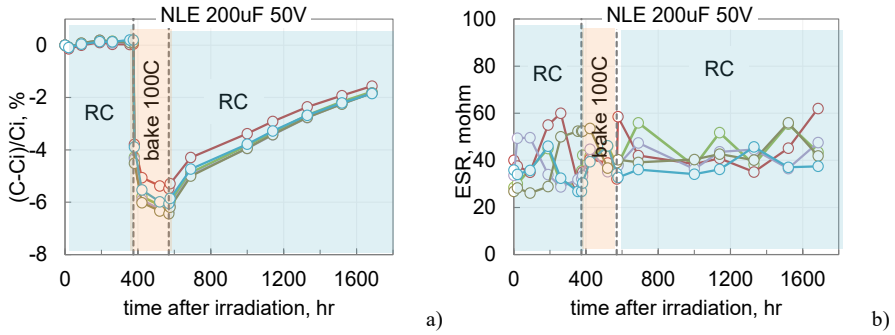

Fig. III.3. Variation of capacitance (a) and ESR (b) in samples from lot 76 irradiated to 5 Mrad over time at room conditions, bake at 100 ºC, and repeat storage at room conditions.

IV. Effect of moisture

Moisture absorption in polymer dielectrics changes characteristics of MPFCs and causes their degradation over time under operating conditions. The first effect is due to increasing dielectric constant and conductivity of polymer materials, while the second is due to corrosion processes in thin aluminum metallization [6, 13, 14]. Usually, the effect of moisture on capacitors is evaluated by storing the parts in humidity chambers, typically at temperatures from 50 to 85 ºC and humidity above 60% RH. These tests showed that the level of humidity has a strong effect on the probability of failures. For example, testing of PP MPFCs at 50 ºC resulted in capacitance parametric failures after 2500 hours at 69% RH, whereas at 79% RH the failure time reduced by a factor of two [15]. In general, failures of MPFCs in power electronic systems are mostly caused by humidity and corrosion [16].

The effect of moisture absorbed in capacitors in room environments is often neglected due to relatively low humidity (30 to 60% RH) and slow processes of moisture penetration for parts encapsulated in plastic. However, because NLEs are not encapsulated, moisture in typical room environments can permeate into dielectric layers relatively easily, and affect both, biased and unbiased behavior of the parts. Encapsulation of NLEs in plastic decreases the rate of moisture diffusion but does not prevent absorption by polymer dielectric layers inside the case. This makes analysis of behavior of NLEs in the presence of moisture important for understanding processes and reliability of fully manufactured capacitors.

1. Variations of AC characteristics

An example of capacitance, and mass variations for several 200 µF and 45 µF NLEs manufactured in 2022 is shown in Fig. IV.1.1. The parts were tested after different bake temperatures and times, storage at room conditions and in a humidity chamber at 85 ºC and 85% RH. Reduction of capacitance caused by 5-7 hours of bake at 150 ºC can reach 7 to 9%. A long-term storage at RC has a tendency of restoring capacitance to the original values.

Assuming that mass changes during bake/storage cycles are attributed to the moisture level in the parts, 45 µF capacitors can contain ~ 1.4 mg of water or 0.4% of the sample mass, and 200 µF capacitors ~ 4.8 mg of water or 0.35% of the sample mass (Fig.IV.1.1.b). After 3 hours in humidity chamber, capacitance increased by 5.3 ±0.5% but all parts fail catastrophically after one week of storage at 85 ºC/85% RH (Fig. VI.1.1.c). As a result, capacitance reduced to 3-6% of the initial value, and ESR increased from ~35 mohm to ohms. Note, that in most cases, an MPFC is considered a parametric failure after losing 5 to 10% of capacitance.

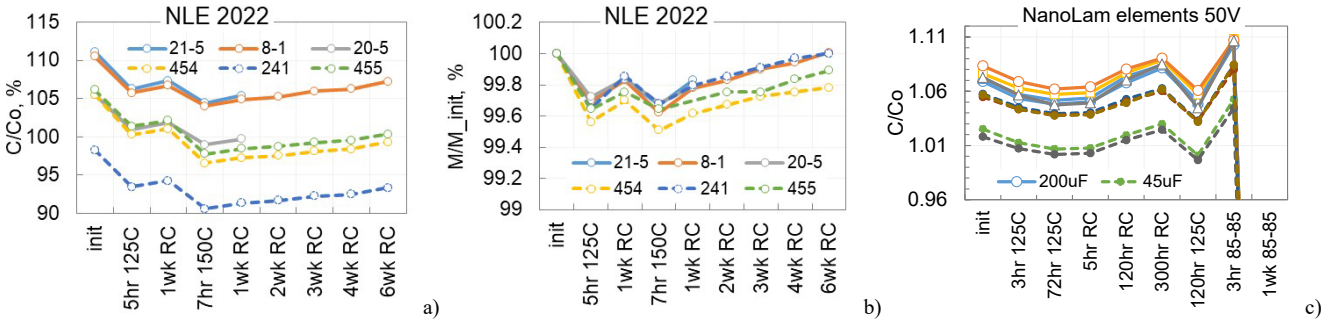

Fig. IV.1.1. Variations of capacitance (a, c) and mass (b) of NLEs during periodical bake at 125 ºC or 150 ºC and storage at room conditions or in a humidity chamber at 85 ºC 85 % RH. Solid lines correspond to 200 µF and dashed lines to 45 µF capacitors.

Cross-sectioning analysis (Fig. IV.1.2) showed that failures in samples exposed to humid environments at 85 ºC and 85% RH for one week were mostly due to corrosion of Al metallization near Zn terminals. The absence of electrical contact at relatively large areas at the terminals resulted in a substantial increase of ESR (from ~30 mohm initially to several ohms after humidity chamber) and decrease of capacitance.

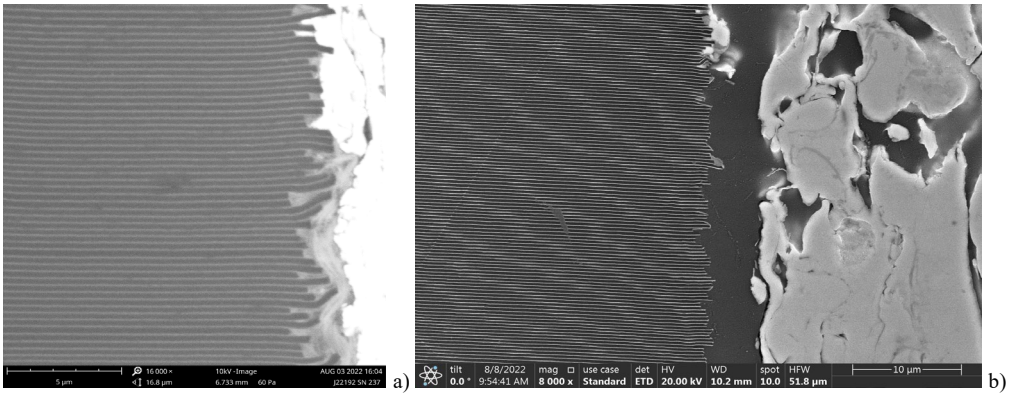

Fig. IV.1.2. Cross-section of an overstressed (a) and humidified (b) samples showing a normal contact between Al electrodes and Zn termination (a) and the absence of connection for a humidified sample (b).

The kinetics of capacitance increase at room conditions after bake at 125 ºC for 24 hours for three NLEs from lots manufactured in 2023 is shown in Fig. IV.1.3a. Capacitance in all elements remained stable for approximately 10 to 20 hours that can be considered as a diffusion delay time. This allowed for measuring AC characteristics for dry NLEs at room conditions. A one-week storage at 20 ºC and 95% RH of a sample from lot 68 resulted in increasing capacitance from 191.6 µF after bake to 207.6 µF after humidification (8% rise). Capacitance in the humidified sample remained stable for ~ 1 hour, but then gradually decreased with time of storage at RC (Fig. IV.1.3.b). Additional tests showed that it takes ~48 hours to dry out NLEs and stabilize capacitance at minimal values in the process of baking at 85 ºC and ~ 10 to 20 hours for baking at 125 ºC.

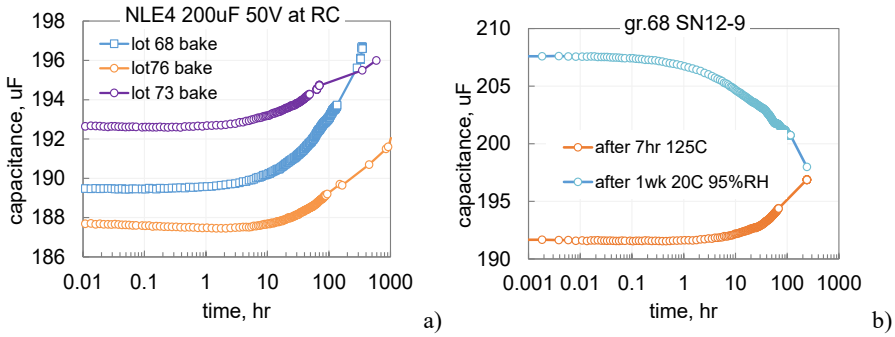

Fig. IV.1.3. Kinetics of capacitance variations at room conditions after bake (a) and different preconditioning (b) for NLEs manufactured in 2023.

The effect of 24-hour bakes at 125 ºC on electrical characteristics of different lots of capacitors (5 samples in a group) is summarized in Table IV.1. Before the bake, these parts were stored at RC for a few weeks. Values of leakage currents during polarization at VR, DCL_p, and depolarization at 0V, DCL_d, were measured after 1000 sec of electrification. The bake resulted in capacitance decrease on average from 1.45 to 2.9% for different lots. Polarization leakage currents decreased from 2 to 5 times, but depolarization currents remained stable. A high sensitivity of leakage currents to the presence of moisture in NanoLam capacitors was also reported by Sandia [17]. The last row in Table IV.1 shows an increase in capacitance for the baked parts after long-term (more than 1000 hour) storage at room conditions. The increase in capacitance is 2 to 2.5 times greater than the decrease caused by the bake shown in the first row. Apparently, the initial exposure to RC was not prolonged enough to saturate samples with moisture.

Variations of capacitance in humid environments is a known effect for MPFCs. The humidity coefficient that is defined as a relative capacitance change determined for a 1% change in humidity varies from 40 to 100 ppm/% RH for polypropylene (PP) capacitors, 500 to 700 ppm/% RH for polyethylene terephthalate (PET) capacitors, and from 700 to 900 ppm/% RH for polyethylene naphthalate (PEN) capacitors [18]. At these coefficients, variations of relative humidity by 50% corresponding to the difference between dry and RC environments, will result in capacitance changes from less than 1% for PP to more than 4 % for PEN capacitors. Considering that more polar polymers can absorb a larger amount of moisture, and the dielectric constant of acrylic polymers used in NLEs is greater than in PP MPFCs, a more significant variation of capacitance in humid environments for NLEs can be expected.

Table IV.1. Changes of capacitance and leakage currents between room and post-bake conditions.

	Lot 2022	Lot 68	Lot 73	Lot 76
$\Delta C_{RC\text{-}bake}$, % (300-500hr at RC)	-2.4 ±0.6	-2.9 ±0.37	-2.3 ±0.34	-1.45 ±0.17
DCL_p_bake/DCL_p_init		0.45 ±0.24	0.21 ±0.12	0.57 ±0.35
DCL_d_bake/DCL_d_init		0.96 ±0.04	1.02 ±0.02	0.99 ±0.04
$\Delta C_{bake\text{-}RC}$, % (1000-1500hr at RC)	6.4 ±0.8	6.0 ±0.2	4.4 ±0.5	3.5 ±0.6

Fig. IV.1.4 shows variations of AC characteristics during 100 ºC bake and post-bake storage at room conditions for six samples from lot 68 that have been exposed to RC before bake for more than 3 months. Most changes during bake occurred within first 100 hours and resulted on average in capacitance decrease by 6%, DF increase by 25% and ESR increase by 37%. After 1000 hours of storage at RC, capacitance recovered to 99% of the initial value, while DF and ESR remained practically stable. Results show that approximately 1000 hours is required to stabilize moisture content and capacitance in NLEs at room environments.

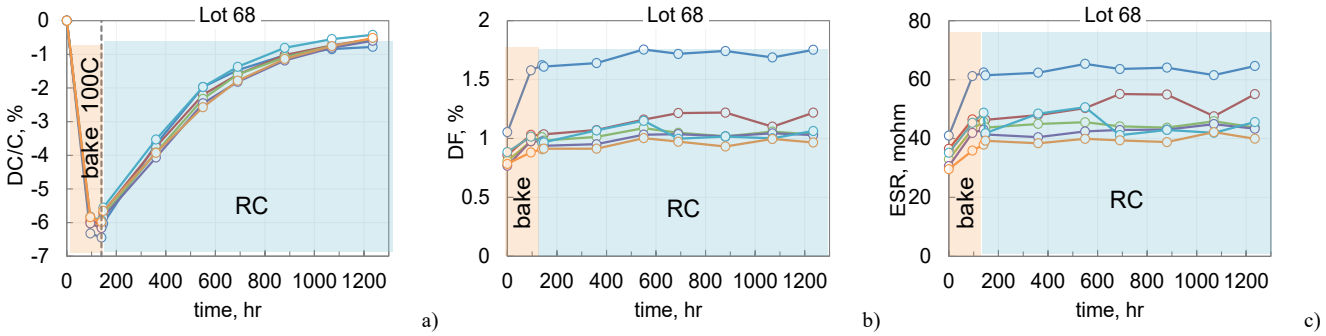

Fig. IV.1.4. Variations of capacitance (a), DF (b) and ESR (c) in six samples from lot 68 during 140 hours bake at 100 ºC and the following storage at room conditions.

2. Biased testing at room conditions

Three samples from each of the lots manufactured in 2023 and one sample of 200 µF capacitors manufactured in 2022 were tested at room conditions and biased at two times rated voltage for 1850 hours. Capacitance and leakage currents were monitored through testing and measurements of capacitance and ESR were continued for 1000 hours more during storage at RC without bias. Results of these tests are shown in Fig. IV.2.1. A sample from lot 2022 had the highest rate of capacitance degradation, 0.053 %/hr, and lost almost 90% of capacitance by 1500 hours. Samples from lots

manufactured in 2023 remained relatively stable for the first 1000 hours when capacitance decreased less than 1%. However, after 1000 hours the rate of degradation increased substantially. By 1850 hours of testing the reduction of capacitance for different lots varied from 4 to 20%. During biased testing, ESR increased by 30% for lot 76 and two times for lot 68 (see Table IV.2.1b).

Surprisingly, the degradation continued even after biased testing when the parts were stored at room environments with no voltage applied. A total decrease of capacitance after 3000 hours of biased and storage testing varied from 8.1 ± 3.7% for lot 76 to 27.5 ± 2.1% for lot 68. A summary of capacitance variations is shown in Table IV.2.1. Apparently, the greater the degradation under bias, the more significant is the decrease of capacitance during storage. Additional rise of ESR caused by storage was maximal, ~30%, for lot 68, ~12% for lot 783 and below 5% for lot 76.

Leakage currents in lots 68 and 73 decreased almost two orders of magnitude during first 400 hours of testing at 100 V (Fig. IV.2.1.c). Elements from lot 76 that had minimal degradation of capacitance had maximal leakage currents that decreased exponentially with time and reduced more than 20 times by the end of testing. A sample from lot 2022 that had maximal capacitance degradation rate, had relatively low leakage currents and a tendency of decreasing with time. Apparently, increased conductivity of NLEs does not indicate a higher rate of capacitance degradation.

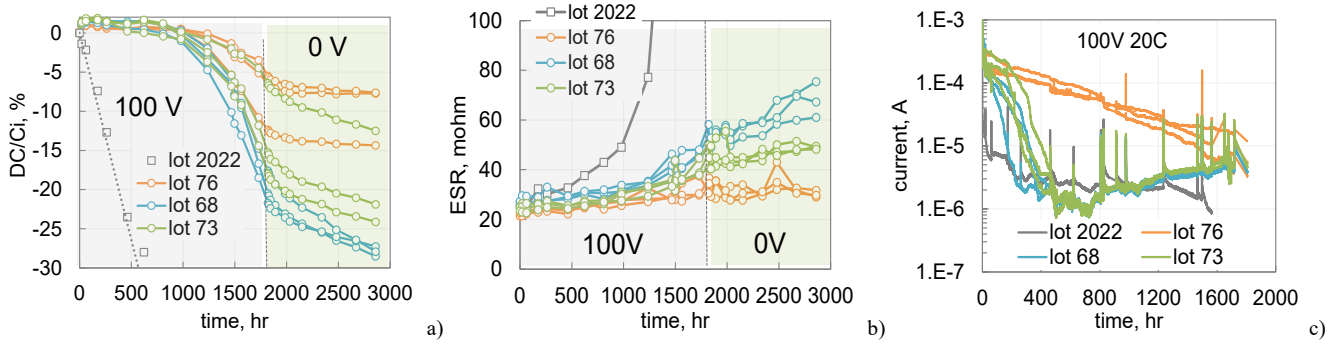

Fig. IV.2.1. Variations of capacitance (a), ESR (b), and leakage currents (c) over time at room conditions under 100 V bias and the following unbiased storage for 200 μF NLEs from different lots. Note, that spikes of the current correspond to times of test interruption for capacitance measurements.

Table IV.2.1. Capacitance decrease after 1850 hours of biased testing at 100 V (% of the initial values) and after the following storage at RC (% of the final values after 1850 hr at 100 V) for three lots of NLEs

	RC, 100 V for 1850hr		RC, storage for 1000hr	
	average	STD	average	STD
Lot 68	-19.9	2.1	-8	2.4
Lot 73	-13.2	6.0	-6.3	0.3
Lot 76	-8.1	3.7	-1.8	0.5

Periodic measurements of depolarization currents during testing at 100 V (similar measurements were also carried out during testing at 125 V that will be described below) showed that samples from all lots had comparable relaxation currents and can be characterized by the same exponent m and absorption capacitance C_t (see Eq. II.1). The exponent m did not change significantly, whereas there was a tendency of increasing C_t with time of testing (Fig. IV.2.2). The higher the level of stress the greater the increase in absorption capacitance, ~40% after 100 V testing, and ~60 % after 125 V testing. These results indicate that new states at the interface Al/polymer can be generated during HALT.

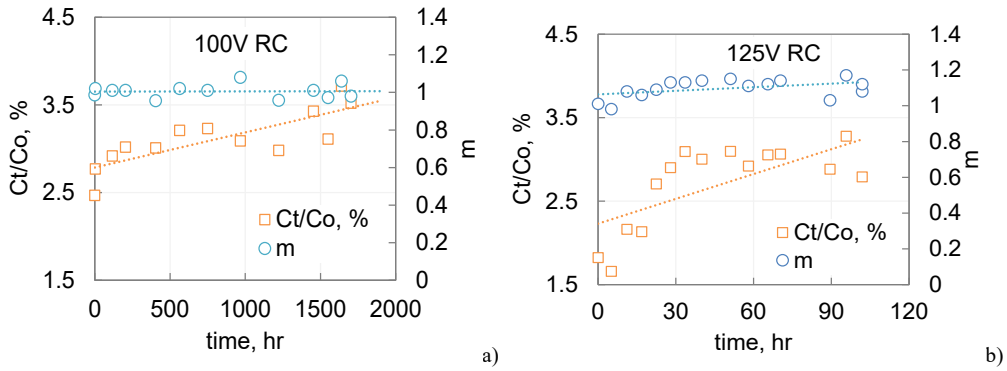

Fig. IV.2.2. Variations of the normalized absorption capacitance and exponent n during testing of NLEs at room conditions and 100 V (a) and 125 V (b).

To assess the effect of the moisture absorbed at room environments on the rate of degradation under bias, two groups of lot 76 elements, with 5 samples each, were tested after different preconditioning. The testing was carried out at room conditions by cycles that included 7 to 20 hours of monitored bias tests at 125 V and 130 to 160 hours of storage either at room conditions (RC group) or at 100 ºC (dry group). Before the first biased test, dry samples were baked for 120 hours. The total time of testing under bias was 140 hours, but the total time of storage between the tests at RC or 100 ºC was 3 months. After 140 hours of biased testing, all parts were baked at 100 ºC for 850 hours and measurements of electrical characteristics continued periodically to assess the possibility of post-electrical-stress degradation for dry and moisture contained parts. Results of these tests are shown in Fig. IV.2.3.

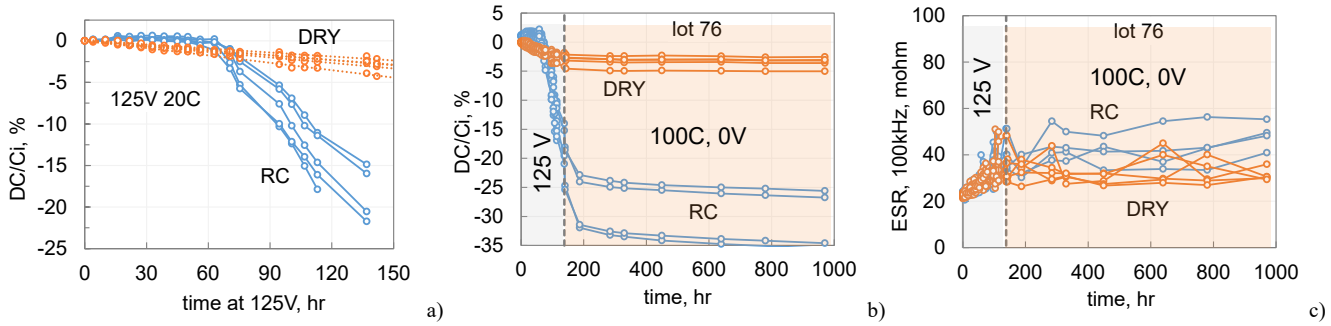

Fig. IV.2.3. Variations of capacitance (a, b) and ESR (c) during testing at room conditions and 125 V for dry and RC capacitors from lot 76. Figure (b) shows changes in capacitance during and after biased testing when the parts stored at 100 ºC.

Capacitance decreased linearly with time for dry parts and by 140 hours reduced on average by 2.7% (Fig.IV.2.3a). Capacitance in RC samples remained stable, and even increased slightly during first 60 hours of testing (corresponds to two months of the intermittent storage), but then the rate of degradation increased substantially, and by the end of electrical testing reduced on average by 20%. Variations of capacitance during electrical testing in RC samples is likely due to two processes related to moisture absorption that acted in opposite directions: (1) increasing of capacitance by rising the effective dielectric constant of polymer dielectrics and (2) corrosion of aluminum metallization that reduces the effective area of metal electrodes. The second process becomes significant after a substantial amount of moisture was absorbed that apparently requires ~1000 hours of exposure to room environments. ESR values during biased testing increased from 20 to 40 mohm for RC group and from 20 to 30 mohm for the dry group, but remained relatively stable during the storage (Fig. IV.2.3.c).

In the process of baking at 100 ºC, capacitance in the dry group decreased slightly, mostly during the first 50 hours, and reduced after 850 hours by 0.85%. The additional drop of capacitance in RC samples was substantially larger, ~16%, and similar to dry capacitors, most of the decrease occurred during first 40 to 60 hours. Variations of capacitance during biased and post-biased baking tests are summarized in Table IV.2.2. The drop in capacitance during bake, 13.3%, is almost 4 times greater than what was assessed as moisture-related changes for lot 76 (Table IV.1) and cannot be explained by moisture desorption. Apparently, most of the degradation was likely due to

aluminum corrosion that continued during the bake. As a result of moisture desorption, corrosion processes were noticeable mostly during first 50 hours, which is close to the expected moisture diffusion time.

Table IV.2.2. Capacitance variations in lot 76 NLEs after 125 V testing and the following bake at 100 ºC.

Precondition	125 V for 140hr at RC		850hr bake at 100 ºC	
	average	STD	average	STD
DRY	-2.7	0.9	-0.85	0.9
RC	-20	3.3	-13.3	4.2

Variations of leakage currents in parts during biased testing at 125 V are shown in Fig. IV.2.4. Overall, currents in dry samples were approximately an order of magnitude lower than for RC samples (Fig. IV.2.3.a). Leakage currents tended to decrease for both groups and had spikes caused by transients that occurred each time the test was interrupted for AC measurements. These transient spikes were different for dry and RC samples as shown in Fig IV.2.2.b. For samples containing moisture, the transients were mostly due to displacement and absorption currents. For dry samples, currents decreased initially but began increasing in approximately an hour of relaxation. Most likely, this was due to moisture absorption in dry samples.

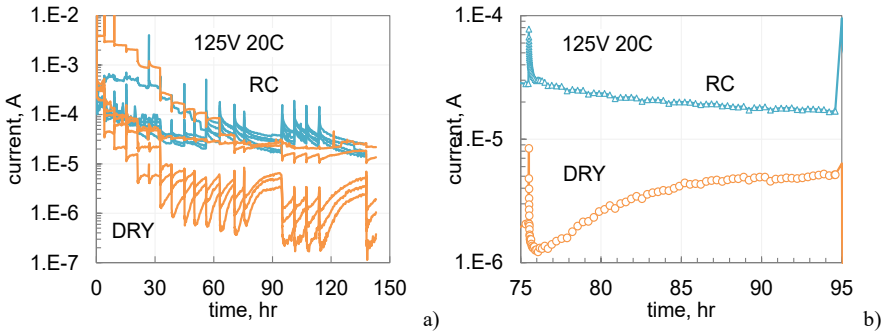

Fig. IV.2.4. Variations of leakage currents during testing at room conditions and 125 V of dry and not-preconditioned (RC) capacitors from lot 76. Figure (b) shows a section of the currents variations for a dry and non-preconditioned samples shown in Fig.(a) for one 20-hour cycle of testing.

As discussed in the previous section, capacitance remains stable in dry samples for at least 10 hours. This indicates that either conductivity of the dielectric layers in NLEs is more sensitive to moisture than the dielectric constant, or the observed increase of currents was due to the surface conductivity at the edges of dielectric layers. The latter is possible if margin areas of NLEs have delamination between the layers allowing for easy penetration for water molecules. The presence of delamination was observed during cross-sectional examinations (see Fig. IV.2.5a) and Fig. IV.2.5b illustrates the possible mechanism of relatively fast-rising currents in NLEs in humid environments.

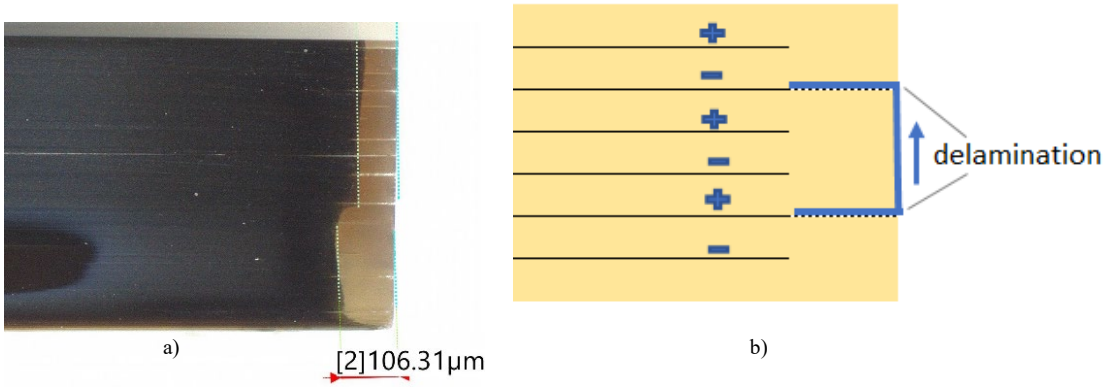

Fig. IV.2.5. Cross-section of an NLE showing delamination in the margin area (a) and schematic of the possible leakage path (b) that can be formed relatively fast in the presence of moisture.

V. Effect of high temperature storage

Reliability of MPFCs is mostly studied under a combination of electrical and temperature stresses, and there is a lack of information on the effect of temperature storage, especially in dry conditions. This might be partially due to a relatively low operating temperature, 105 ºC, of the most popular type, polypropylene (PP) capacitors. The maximum operating temperature for NanoLam capacitors is much higher, 140 ºC, so the effect of high temperature storage (HTS) should be evaluated.

Mechanisms of degradation of MPFCs during storage at high temperatures may be related to processes in polymer dielectrics or in thin aluminum films [19]. The first, can be caused by structural changes in polymers, thermal or thermo-oxidative degradation that can change dielectric constant and conductivity of dielectric layers. The second process might be due to oxidation or corrosion of aluminum that increases ESR and decreases the roll-off frequency; and hence, the capacitance of the parts. Oxidation on a freshly formed aluminum surface in room environments occurs very fast (within seconds) and results in formation of a passivation oxide layer with a thickness of ~ 2 nm. However, a slow oxidation can continue with time increasing the thickness of oxide above 2 nm [20]. This process may have a rather large activation energy of ~ 1.2 eV. Considering a small thickness of Al electrodes, of 10 to 20 nm, may increase the resistivity of aluminum layers.

Evaluation of the effect of HTS on NLEs, was carried out by periodic measurements of the characteristics of parts with time of storage at 125 ºC (HTS125). To assess the effect of defects or damage created by self-healing or exposure to high humidity, three sub-groups of 45 µF and 200 µF capacitors manufactured in 2022 were used. One subgroup had virgin samples, another was samples overstressed at 150 V for 28 hours, and the third was comprised of samples that failed after storage in at 85 ºC 85% RH for 1 week (see Fig.IV.1.1).

Frequency dependencies of capacitance and ESR for the three groups before HTS125 are shown in Fig. V.1. Capacitance in overstressed samples was reduced by ~25% compared to virgin samples, and in the parts failed catastrophically after humidity chamber the reduction was ~ 95%. Contrary to relative capacitance variations that were similar for 200 µF and 45 µF parts, ESR increased for overstressed NLEs in ~2 times for 200 µF and 4.5 times for 45 µF samples. In parts after humidity chamber, the rise of ESR was 83 and 125 times for 200 µF and 45 µF parts respectively. It is possible that a larger concentration of defects (delamination) in 45 µF capacitors allowed for a faster penetration of moisture to metal electrodes and resulted in a more significant degradation caused by corrosion of aluminum metallization near terminals.

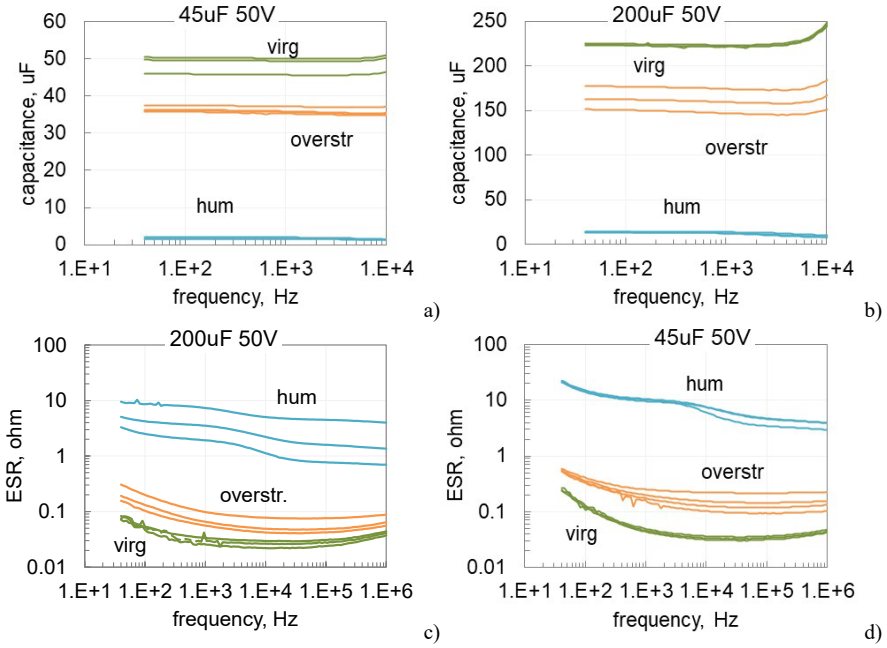

Fig.V.1. Frequency variations of capacitance (a. c) and ESR (b. d) for different groups of NLEs before high temperature storage.

Results of periodic measurements of capacitance, ESR, and leakage currents at room temperature during 4000 hours of HTS125 are shown in Fig.V.2. The initial drop of capacitance in virgin samples measured after 120 hr of HTS125 was 6.4 ±0.85% and as shown in the previous section was due to moisture desorption. This drop was much larger for "humid" capacitors, 15 ±3%, and for overstressed parts, 10 ±3.9%. A higher decrease of capacitance for humidified compared to virgin samples might be expected, but a larger decrease in the overstressed samples might indicate a larger accumulation of moisture in samples with multiple self-healed areas. It is possible that self-healing results in formation of micro-voids that facilitate degradation processes. Additional tests showed that voltage overstressing results in bulging of the surface of NLEs that indicates the presence of voids between the dielectric layers.

After 120 hours, additional degradation of capacitance by 4000 hours was on average 2.3 ±1.2% for virgin samples, 5.4 ±3.5% for the overstressed samples, and 12 ±8.5% for humidified samples. Degradation of ESR was relatively small for virgin parts (~45%), much more significant (~27 times) for the overstressed capacitors, and ~2 times for humidified parts. The latter was apparently due to much greater initial values of ESR for these parts. A more significant degradation of AC characteristics for the overstressed and humidified parts indicates that the preexisting damage to aluminum metallization can further develop during unbiased storage in dry conditions. Most likely, this degradation was due to oxidation or corrosion of thin aluminum metallization that was spreading from the initially damaged areas.

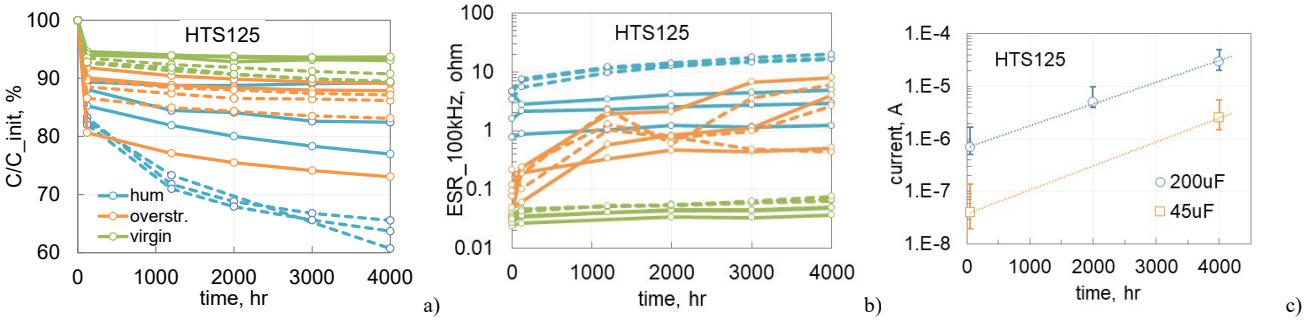

Fig.V.2. Degradation of normalized capacitance (a), ESR (b), and leackage currents (c) in the during HTS125. Green lines correspond to virgin, blue for parts after hunmidity chamber, and orange for the overstressed NLEs; solid lines represent 200 µF and dashed lines 45 µF samples.

Leakage currents in virgin NLEs measured after 1000 sec of electrification (Fig. V.2.c) increased after HTS125 by more than an order of magnitude. To get a better understanding of the degradation mechnism, voltage dependencies of currents and long-term variations of currents at RC after 4000 hours of HTS125 were measured. Results in Fig. V.3.a indicate a decrease in the shottky barrier at the aluminum/polymer interface after HTS. The barrier apparently rises to the initial level after a dozen of hours of electrification at room conditions and 50 V (see Fig. V.3.b). As apparent from Fig. V.3c, HTS125 did not cause significant changes in the absorption currents. Similar results of reversible increasing of leakage currents after HTS were observed in aluminum and tantalum electrolytic capacitors and were explained by capturing/releasing of electrons from the deep states in the dielectric [21]. Apparently, a similar mechanism can be used to explain behavior of MPFCs.

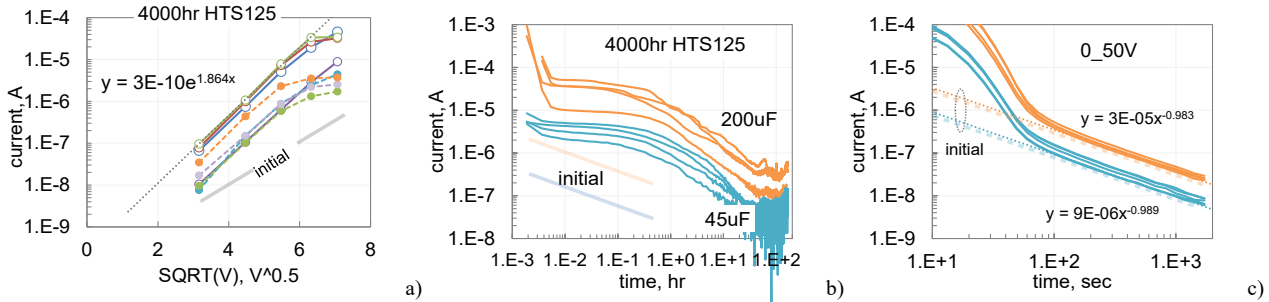

Fig.V.3. Leakage currents before and after 4000 hours of HTS125. (a) I-V characteristics based on 1000 sec current measurements; (b) variations of leakage currents with time during 100-hour testing at 20 ºC and 50 V after HTS125; (c) depolarization currents after 100-hour testing. Dashed lines in Fig.V.3a correspond to 45 µF and solid lines to 200 µF capacitors.

VI. Highly Accelerated Life Testing

1. Leakage currents during HALT

HALT of 200 µF and 45 µF capacitors manufactured in 2022 started as a step stress test at 100 V with 100-hours steps at 85 ºC, 105 ºC, 125 ºC, and 145 ºC. After that, HALT continued till 1000 hours at 145 ºC. The parts were periodically cooled down to room temperature for measurements of AC characteristics. No failures were observed, and there was a trend of reducing currents over time during HALT. This reduction was especially significant, approximately two orders of magnitude, during the first 100 hours of tests as shown in Fig. VI.1.1. Currents up to 1 hour of testing at 85 ºC remained relatively large but then reduced ~ 50 times by 100 hours. This was likely due to moisture remaining initially in the samples. As was shown above, it takes ~48 hours for moisture desorption at 85 ºC, whereas at 125 ºC this may happen within hours. The currents continue reducing after the first cycles of HALT as shown for 1000-hour testing at 145 ºC and 100 V in Fig. VI.1.1.d. On average, currents reduced by the end of HALT by 2.5 times compared to 100-hour measurements.

Reduction of currents with the time of HALT after moisture desorption might be attributed to self-healing processes in the dielectric that effectively isolate local defect areas with high conductivity. Another, and more likely reason, is increasing of the barrier at the polymer/aluminum interface caused by electrons' trapping at the deep states in the dielectric similar to processes in Al2O3 and Ta2O5 dielectrics in electrolytic capacitors [21].

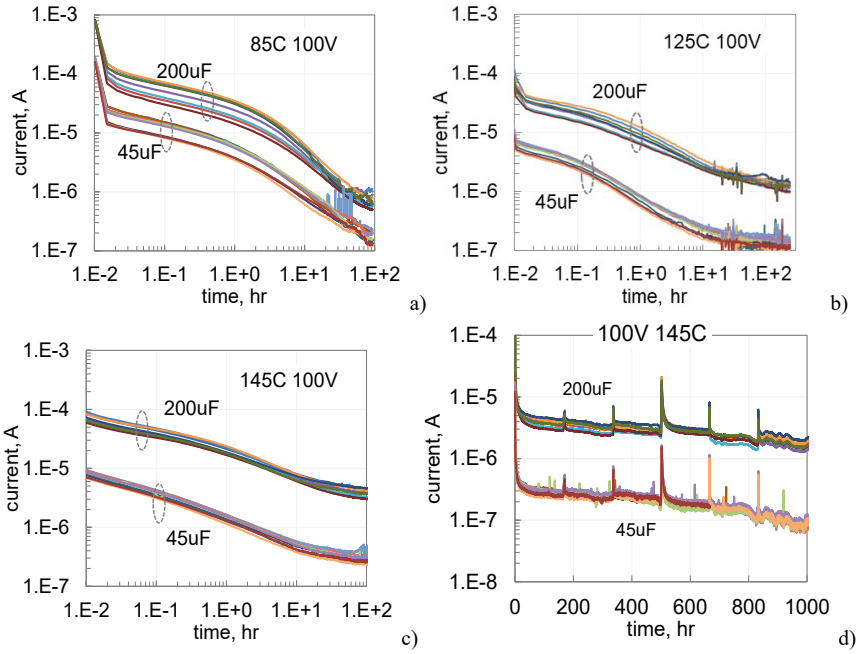

Fig. VI.1.1. Leakage currents during the first 100 hour cycle of HALT at 100 V in lot 2022 elements at temperatures of 85 ºC (a), 125 ºC (b), 145 ºC (c), and 1000-hour HALT at 145 ºC.

Currents in 200 µF capacitors were greater than in 45 µF parts at 85 ºC on average in 4.5 times that corresponds to the difference in capacitance values. However, the difference at 125 ºC and 145 ºC was more than 10 times. Assuming that both parts are manufactured using the same materials and processes, the reason for this difference is not clear.

Several samples had unstable currents during HALT as shown in Fig. VI.1.2a-c. However, the level of leakage currents and anomalous behavior reduced by the end of HALT when samples were tested at 20 ºC and rated voltage (Fig. VI.1.2c). This result is likely due to a better clearing of poorly cleared defects with time of electrical stress. Although the parts with unstable leakage currents had normal AC characteristics and the level of currents at room conditions, they should have been screened out during burn-in testing.

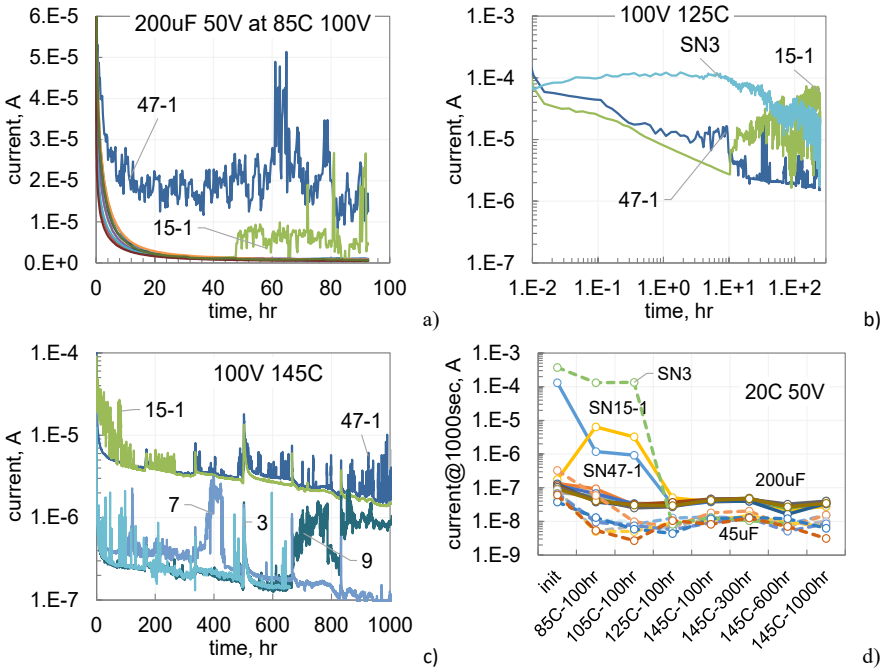

Fig.VI.1.2. Unstable leakage currents in three samples during testing at 100 V and 85 ºC (a), 125 ºC (b), and 145 ºC (c). Figure (d) shows currents measured periodically through the step stress and HALT testing at 20 ºC and 50 V.

A reduction of leakage currents was also observed in 200 µF capacitors from lot 2022 during long-term high voltage stress testing at room conditions (see VI.1.3). Voltage dependencies of leakage currents (see Fig. VI.1.3d) indicate Schottky conduction mechanism, so similar to results of HALT, the observed reduction of leakage currents might be explained by increasing the barrier at the aluminum/polymer interface as a result of trapping of charge carriers in the dielectric.

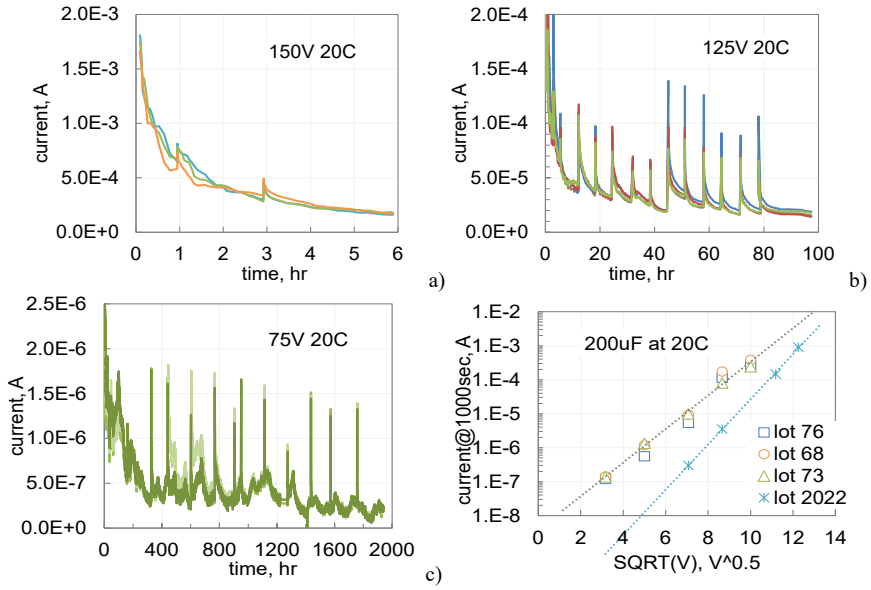

Fig. VI.1.3. Leakage currents in 200 µF NLEs during stress testing at 20 ºC and 150 V (a), 125 V (b), and 75 V (c). Figure (d) shows voltage dependencies of median leakage currents measured after 1000sec of polarization in Schottky coordinates for different lots of capacitors used in this study. Current spikes on charts (a-c) were due to test interruptions for measurements of AC characteristics.

Leakage currents during 1000-hour HALT at 100 V and 120 V and temperatures 85 ºC and 125 ºC for lots manufactured in 2023 are shown in Fig. VI.1.4. Before testing, the parts were baked at 125 ºC for 24 hours. In all cases, similar to parts from lot 2022, leakage currents decreased with time under bias. Lot 76 had approximately an order of magnitude higher leakage currents compared to other lots. At 85 ºC, currents in lots 68 and 73 were stabilizing at the sub-microampere levels after 200 to 400 hours, whereas in lot 76 exponential decrease continued for more than 1000 hours.

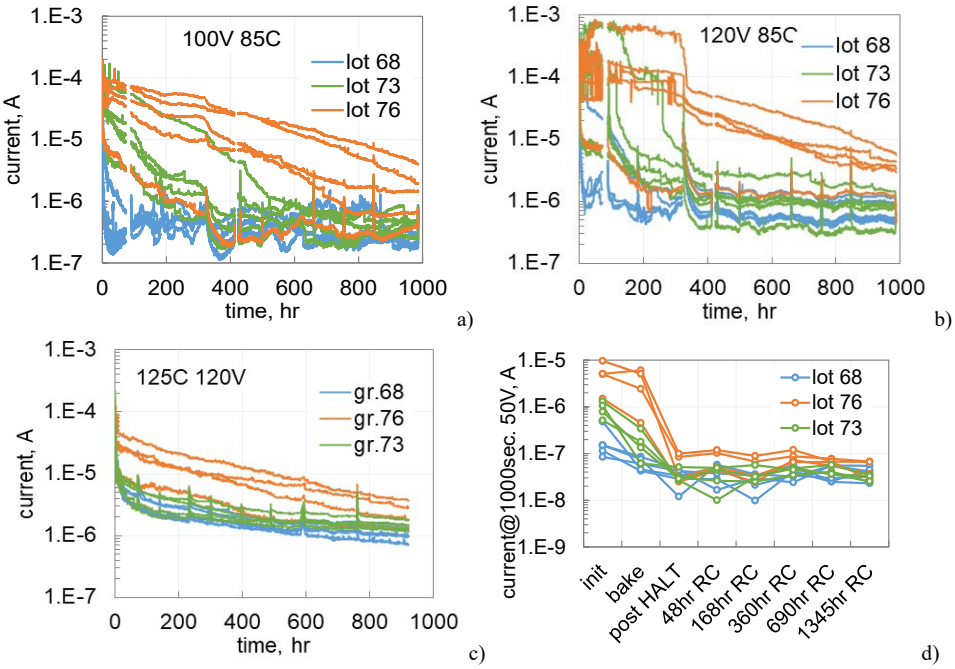

Fig. VI.1.4. Leakage currents in three lots of 200 µF NLEs during HALT at 100 V and 85 ºC (a), 120 V and 85 ºC (b), and 120 V and 125 ºC (c). Figure (d) shows leakage currents measured at 50 V and room temperature after 1000 sec of electrification at different states through the testing.

After HALT, measurements of leakage currents were repeated periodically up to 1345 hours of storage at room conditions. Results in Fig. VI.1.4d show that the currents at 50 V decreased 2-3 times after bake, and up to two orders of magnitude after HALT. The following storage at room conditions that may increase conductivity due to moisture absorption, did not change currents significantly after four weeks of storage. Apparently, changes in leakage currents caused by the increase of the barrier are more significant compared to the effect that can be caused by moisture absorption.

2. Degradation of AC characteristics during HALT

Degradation of capacitance, DF, and ESR for 200 µF NLEs manufactured in 2022 in the process of testing at room conditions and voltages of 75 V, 125 V, and 150 V (1.25VR to 3VR) are shown in Fig.VI.2.1. In all cases capacitance variations with time can be approximated with straight lines with slopes indicating the rate of degradation, *r*. Values of DF and ESR were also degrading with time, but the spread of data is much greater than for capacitance.

To assess the effect of self-healing on the rate of degradation, testing at 75 V was carried out using a group of virgin parts and a group of samples stressed for 6 hours at 150 V (see Fig. VI.2.1.g-i). The initial drop in capacitance for the stressed parts was greater; however, the rate of degradation for these samples measured after the initial drop was 1.2E-5 ±2.9E-6 1/hr, which is ~80% lower compared to the virgin samples (12.2E-5 ±2.8E-6 1/hr). This may indicate a reduction of the degradation rate with time under stress. However, a relatively small sample size used in this experiment requires additional testing to confirm the effect.

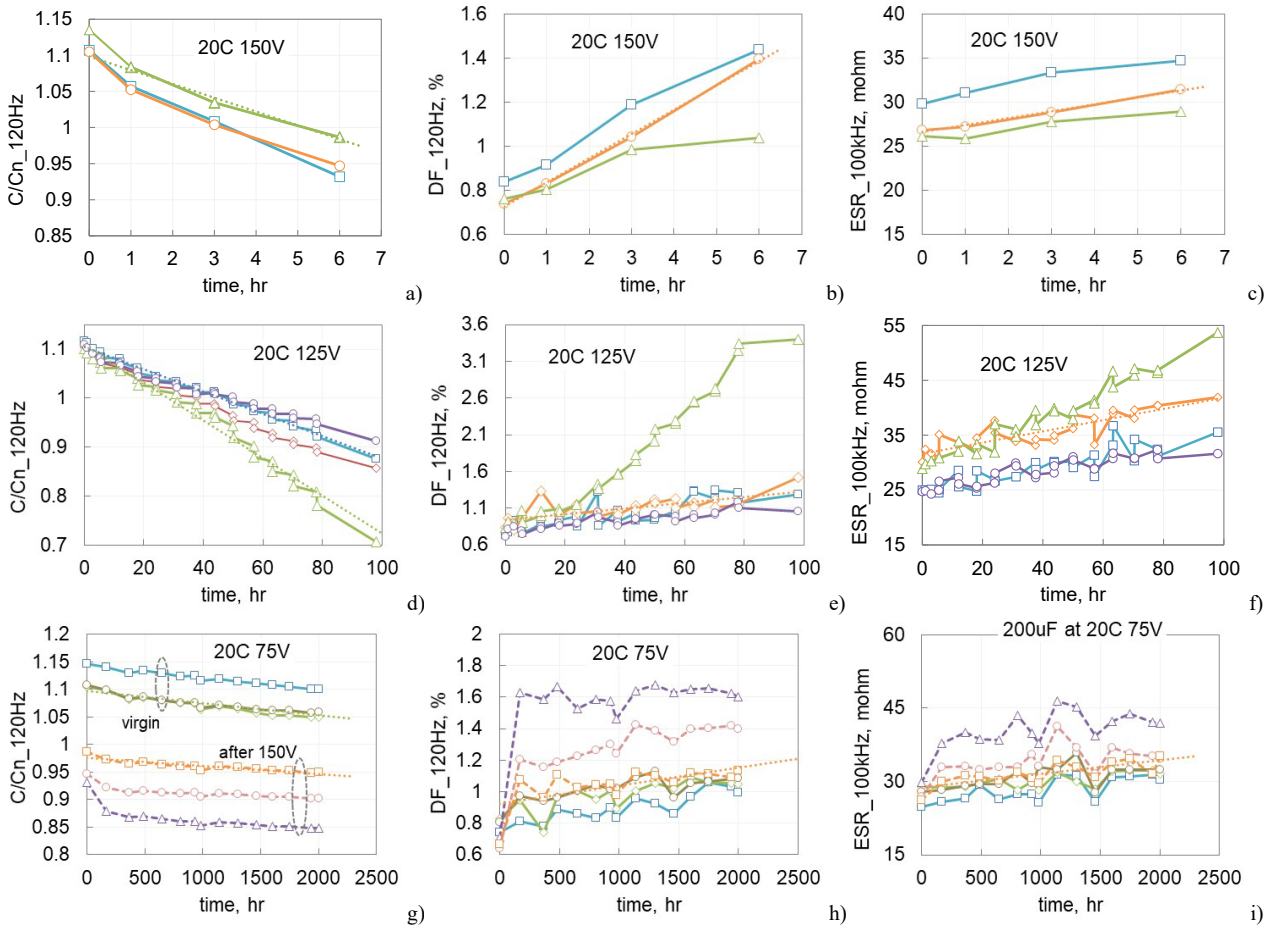

Fig.VI.2.1. Degradation of AC characteristics in 200 µF NLEs at 20 ºC and voltages of 150 V (a-c), 125 V (d-f) and 75 V (g-i).

Average values of the rate of capacitance degradation are plotted against normalized stress voltage in Fig. VI.2.2. The results indicate a strong voltage dependence that can be approximated by a power function with an exponent of 9.8. This approximation allows calculating the rate of degradation at 100 V: r = 3.7E-4 1/hr. This result is consistent with data from experiments described in section IV.2 where the rate of degradation for a single sample tested at 100 V was 5.3E-4 1/hr. Using this approximation, the rate of degradation at the rated voltage is 4E-7 1/hr, and the time to failure that is defined as 10% loss of capacitance is 28.5 years at room conditions. Derating of voltage to 0.6VR will increase this time to more than 4200 years.

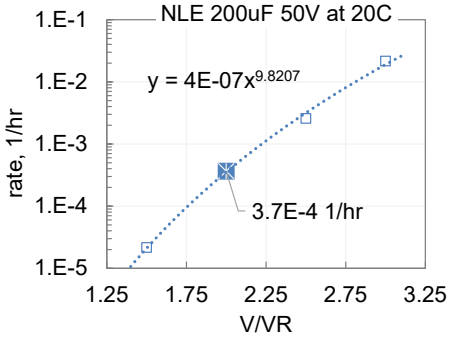

Fig. VI.2.2. Voltage dependence of the degradation rate for a lot 2022 of 200 µF 50 V NLEs tested at room conditions. Asterisk indicates degradation rate calculated at 100 V.

Variations of normalized capacitance during HALT at 145 ºC and 100 V for 200 µF and 45 µF samples from lot 2022 are shown in Fig.VI.2.3a. Distributions of the degradation rates (Fig. VI.2.3b) are similar for both types of the elements. Increasing stress voltage from 75 to 100 V at 85 ºC increased the rate of degradation for 200 µF capacitors almost three times, from 3.74E-5 1/hr to 1.07E-4 1/hr (see Fig.VI.2.3c). Note, that the degradation rate at 100 V and 85 ºC is almost five times lower than at room conditions. This can be explained considering the effect of moisture on the degradation processes in NLEs.

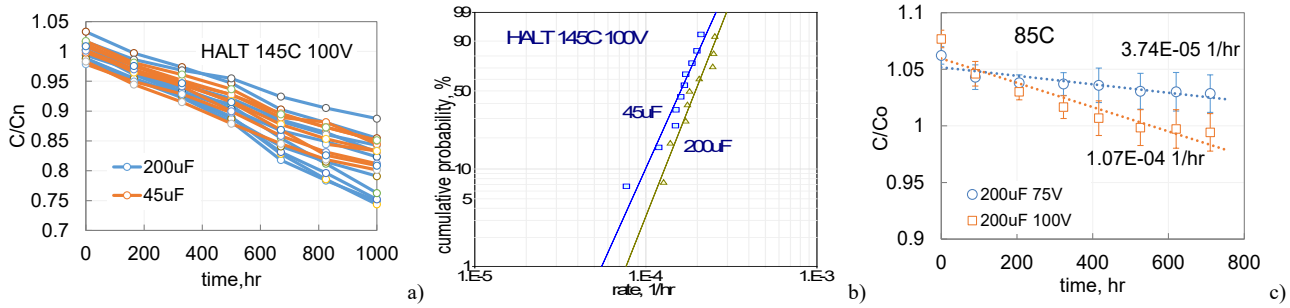

Fig.VI.2.3. Variations of normalized capacitances with time during HALT at 145 ºC and 100 V (a), distributions of the degradation rates for 200 µF and 45 µF capacitors (b), and degradation of capacitance at 85 ºC and two stress voltages, 75 V and 100 V (c).

Degradation of capacitance in three lots of NLEs manufactured in 2023 during HALT at 85 ºC and 125 ºC and voltages 2VR and 2.4VR is shown in Fig. VI.2.4. Variations of capacitance can be accurately enough approximated with strait lines allowing for calculations of times to failure (*TTF = 0.1/r)*. In spite of a relatively small sample size (5 samples in a group), results show difference in reliability of different lots of NLEs. Degradation rates during testing at 125 ºC and 120 V were greater for lot 68, 2.2E-4 ±4.5E-5 1/hr, compared to lot 73, 1.4E-4 ±2.5E-5 1/hr, and lot 76, 1E-4 ±1.8E-5 1/hr.

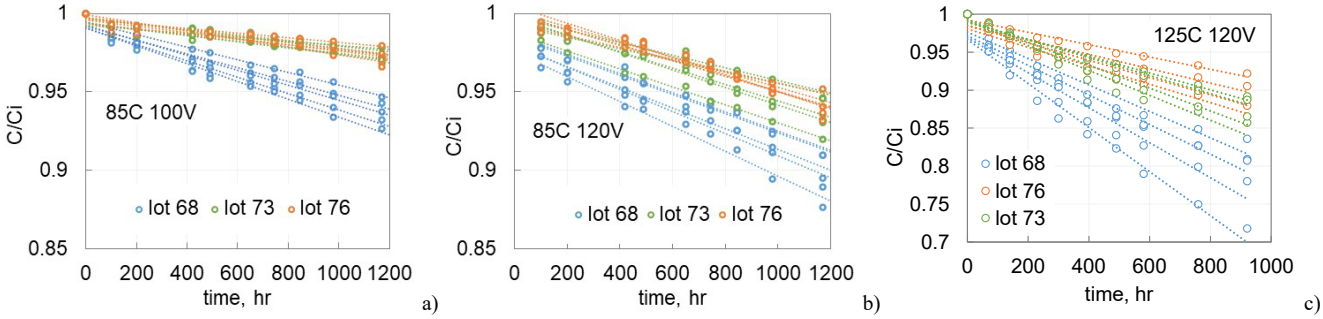

Fig.VI.2.4. Degradation of capacitance in three lots manufactured in 2023 during HALT at 85 ºC 100 V (a), 85 ºC 120 V (b), and 125 ºC 120 V (c).

To evaluate stability of characteristics after HALT, capacitance measurements were continued for up to 2000 hours of storage at room environments. Results of these measurements are shown Fig. VI.2.5 and summarized in Table VI.2. Contrary to storage of samples after biased testing at room conditions, where capacitance continued decreasing with time after electrical stress, post-high-temperature-HALT samples showed increasing of capacitance with time (up to ~6%). Before increasing, similar to results shown in Fig. IV.1.3, capacitance remained relatively stable for up to 10 hours (see Fig.VI.2.5a, b). The post-HALT variations of capacitance are consistent with the effect of moisture sorption discussed above: ~10 hours diffusion delay, and the range of capacitance increase from 4 to 6 %.

Apparently, capacitance degradation during HALT for dry samples is mostly due to self-healing processes that stop with the voltage stress. For these samples, increasing of capacitance caused by moisture absorption after HALT is more significant compared to possible moisture-induced degradation. Contrary to that, samples containing moisture during HALT, degrade further due to corrosion processes that continue during storage, although at a lower rate.

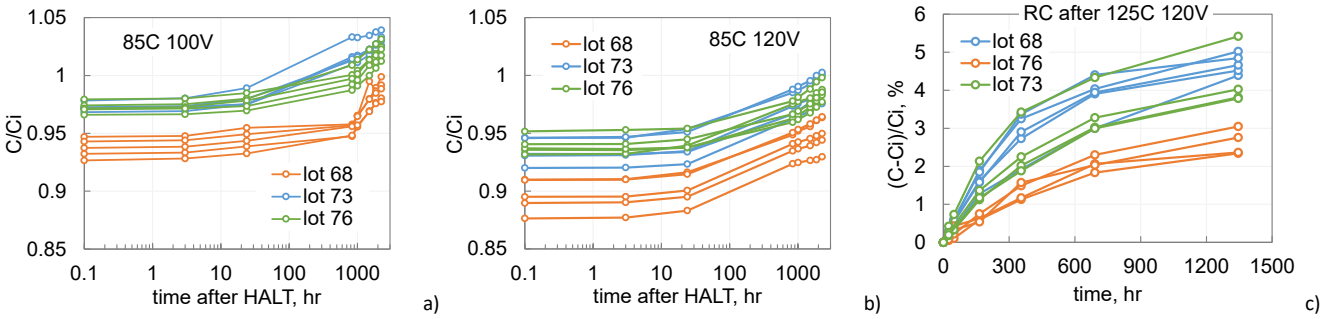

Fig.VI.2.5. Variations of capacitance with time at room conditions after HALT in three lots shown in Fig. VI.2.4; post HALT at 85 ºC 100 V (a), 85 ºC 120 V (b), and 125 ºC 120 V (c).

Table VI.2. Increase in capacitance during storage at RC for 2300 hours following HALT at 100 V and 120 V, and after 1345 hours following HALT at 125 ºC, 120 V.

	85C/100V		85C/120V		125C/120V	
	ΔC, % avr	STD	ΔC, % avr	STD	ΔC, % avr	STD
Lot 68	5.0	0.16	5.4	0.06	4.7	0.25
Lot 73	5.9	0.2	5.5	0.12	4.3	0.78
Lot 76	4.9	0.5	4.7	0.6	2.6	0.34

3. Reliability acceleration factors

Assuming that failures of NLEs occur when capacitance decreases to 90% of the initial value, the times to failure (TTF) were determined either directly from the test data for samples with $C(t)/C_i < 0.9$ or calculated for each sample as $TTF = 0.1/r$, where r is the rate of degradation. The values of r were calculated as slopes of trend lines similar to those shown in Fig.VI.2.4.

Distributions of *TTF* were approximated with Weibull functions:

$$F(t) = 1 - exp\left[-\left(\frac{t}{TTF_c}\right)^{\beta}\right], \quad \text{(VI.1)}$$

where $F(t)$ is the probability of failure at time t, TTF_c is the characteristic time to failure (scale parameter), and β is the shape parameter (slope) of the distribution. Distributions of TTF with $\beta < 1$ indicate infant mortality (IM) failures and with $\beta > 1$ wear-out (WO) failures.

Variations of the characteristic times with voltage and temperature were approximated with a general Weibull log-linear model:

$$TTF_c = A \times exp\left(\frac{E_a}{kT}\right) \times V^n \ , \quad \text{(VI.2)}$$

where A, E_a, and n are constants, k = 8.617E-5 eV/K is the Boltzmann's constant, and T is the temperature.

ALTA-7 software available from ReliaSoft was used to calculate parameters of the model based on the maximum likelihood estimations (MLE).

Reliability of components failing due to wear out (WO) processes cannot be characterized by the failure rate only. It is also important evaluate the useful time, or time to the inception of WO failures, TTF_i. This time can be determined as a time when the probability of failure at operating conditions increases to 1% and can be calculated using a Weibull function:

$$TTF_i = TTF_c \times [-\ln(0.99)]^{1/\beta} \ , \quad \text{(VI.3)}$$

Results of approximation of TTF distributions for 200 µF NLEs from lot 2022 are shown in Fig.VI.3.1. Simulations based on testing at room environments (Fig. VI.2.1) resulted in β = 3.5 which indicates WO failures of the parts. The

voltage acceleration constant was rather large, $n = 9.5$ and the useful life at 30 V (0.6VR) and 20 ºC exceeds 900 years. Simulations using results at different temperatures and voltages (Fig. VI.2.3) resulted in a similar large value of n = 8.7 and relatively small activation energy, $E_a \sim 0.12$ eV. The slope of the distributions, $\beta = 1.5$, also indicates were-out failures. In spite of a relatively small sample sizes and spread of the data, modeling allows for reliability assessments for the use conditions. Calculations show that 99% of the part will have TTF more than 80 years during operations at 30 V and 65 ºC (Fig. VI.3.1.b).

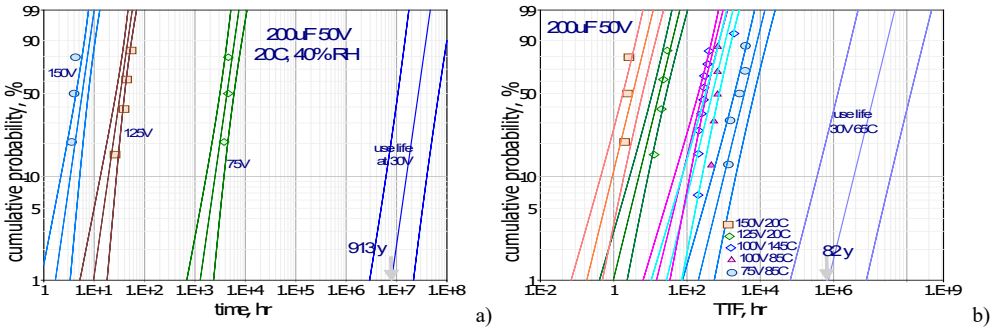

a) b)

Fig.VI.3.1. Weibull distribution of times to failure for 200 µF elements (lot 2022) at 20 ºC (a) and at different temperatures and voltages (b). Marks indicate experimental data, lines are approximations based on the general Weibull log-linear model, and dotted lines are 90% confidence bounds.

Comparison of TTF values for the four lots of 200 µF NLEs tested at room conditions and 100 V is shown in Fig. VI.3.2a. Although only one sample from lot 2022 was tested, it is expected that the distribution of TTF will have a slope similar to distributions shown in Fig. VI.3.1a, $\beta = 3.5$. Based on the acceleration factors calculated for data in Fig.VI.3.1a, the mean life at 100 V is 277 hours that is close to 220 hours for the sample presented in Fig. VI.3.2a. Results show that different lots of NLEs might have substantially different reliability at room conditions when failures are most likely due to the presence of moisture and corrosion of aluminum metallization.

TTF distributions based on test results at room conditions for samples from lot 76 that were described in section V are shown in Fig. VI.3.2.b. One of the two groups tested at 125 V was preconditioned by bake at 100 ºC for 120 hours and then stored between tests also at 100 ºC (dry samples), whereas another remained at room conditions with the moisture level corresponding to room environments (RC samples). The characteristic time of failures for dry capacitors is more than five times greater than for RC samples. Similar to results shown in Fig.V.3.1a, test voltage had a strong effect on TTF distributions. For samples without preconditioning, TTF_c decreased from 2120 hours at 100 V to 103 hours at 125 V that corresponds to n = 13.5. The expected useful life (time to 1% failures) for these parts at 30 V and room conditions exceeds 1000 years.

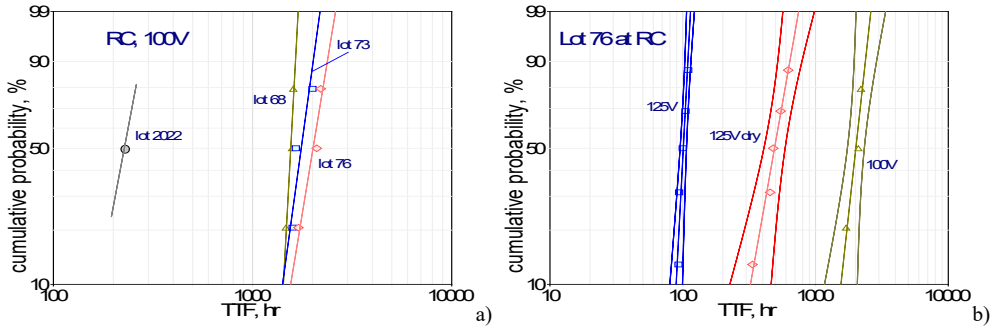

a) b)

Fig.VI.3.2. Times to failures at room conditions for four lots of NLEs during 100 V testing (a) and the effect of bake on TTF distributions at RC for lot 76 (b). Group "125 V dry" corresponds to samples baked at 100 ºC before and through the testing, whereas samples marked "125 V" and "100 V" were tested without preconditioning.

Distributions of TTF calculated based on results of HALT at high temperatures shown in Fig.VI.2.4 for the three lots manufactured in 2023 are shown in Fig. VI.3.3. Parameters of the log-linear models per Eq.(VI.2) are summarized in Table VI.3. Despite a small sample size used for HALT, results show a substantial difference in reliability between

four different lots of NLEs. Predictions for the useful life assuming operation at 65 ºC and 30 V give more than 1000 years for lots 73 and 76, but only 9.5 years for lot 68.

Voltage acceleration constant, n, was large, and except for lot 68 was in the range from 6.3 to 8.6 and the activation energy, E_a, was relatively low, below 0.5 eV. Respectively, voltage derating will have a more significant effect on reliability compared to temperature derating. For example, decreasing temperature from 85 to 65 ºC will increase useful life in less than 2.5 times, whereas decrease of voltage from 0.6VR to 0.5VR will increase the time to failure inception from 3.1 to 4.8 times.

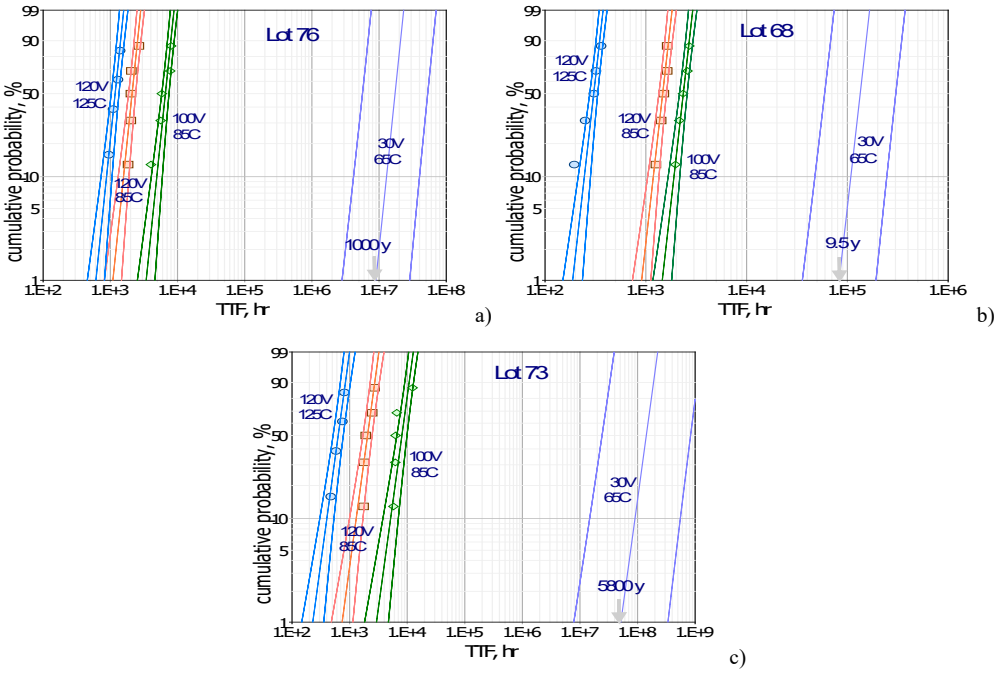

Fig. VI.3.3. Weibull distributions of TTF calculated based on HALT at 85 ºC 100 V and 120 V and at 125 ºC 120 V for lot 76 (a), lot 68 (b), and lot 73 (c).

The values of the voltage reliability acceleration constants obtained for NLEs are withing the range of values calculated for conventional MPFCs based on data presented by manufacturers [22-26]. The reported data indicate a wide range for n, from 1.8 to 19. The activation energy is also changing in a wide range, $0.6 < E_a < 3.6$ eV, which is larger than our assessments. Note, that according to MIL-PRF-83421 all types of MFPCs have voltage acceleration factor, $AF_V = 5$, at 105 ºC and 1.4VR, which corresponds to $n = 4.8$. MIL-PRF-19987 specifies that $AF_V = 5$ for $V_{op} > VR$ and $AF_V = 4$ for $V_{op} < 0.9VR$. Based on multiplying factors for the failure rates, the activation energy varies from 0.55 eV at 0.6VR to 0.49 eV at 1.4 VR. Apparently, reliability acceleration factors are specific to a certain technology and design of MPFCs and application of generic data to reliability assessments of NanoLam capacitors might be misleading. Insufficient control over the moisture level in the parts can also result in substantial variations in reliability characteristics. Additional testing of assembled capacitors in dry conditions are necessary to predict reliability of the parts for space applications.

Table VI.3. Parameters of TTF distributions and predictions for useful life for different lots of NLEs.

	Lot 2022		Lot 68	Lot 73	Lot 76	
	RC	HT	HT	HT	RC	HT
β	3.5	1.5	8.8	4.2	15	6.4
n	9.5	8.6	2.6	7.5	13.5	6.3
E_a, eV		< 0.01	0.48	0.36		0.18
TTF_i at 20C/30V, years	913				2E6	
TTF_i at 65C/30V, years		82	9.6	5800		1000

VII. Summary

Characteristics of NLEs and their degradation depend on the amount of moisture absorbed in the dielectric. Exposure to humid environments, including room conditions, should be thoroughly controlled during manufacturing and testing of the elements, processes of assembly and encapsulation at the final stages of capacitors' manufacturing, and prevented during the following storage and ground phase integration and testing periods.

1. Radiation testing.
   a. Radiation testing at the rate of 39 rad/sec caused a relatively minor degradation of AC and DC characteristics: after irradiation to 5 Mrad Si capacitance increased less than 5%, DF less than 38%, and ESR less than 93%. Leakage currents decreased almost an order of magnitude and absorption capacitance decreased ~2.5%.
   b. The observed changes were mostly due to moisture sorption during periods of storage of NLEs at room environments between incremental radiation exposures.
2. Storage at room conditions.
   a. Moisture sorption at room environments resulted in reversible variations of capacitance that for different lots of NLEs varied on average from 3.5 to 6.4%.
   b. Bake-out times are decreasing from ~48 hours at 85 ºC to ~20 hours at 125 ºC. Incubation period at room conditions after bake and before the moisture-related increase in capacitance is ~ 10 hours.
   c. Exposure of NLEs to humidity at 85 ºC and 85% RH for one week can cause catastrophic parametric failures: reduction of capacitance to 3-6% of the initial value and increase of ESR from dozens of milliohms to a few ohms. The failures were due to corrosion of aluminum metallization near the terminals.
   d. Leakage currents in dry samples are 2 to 5 times lower compared to samples saturated with moisture at room environments. After bake, leakage currents at room conditions are increasing within hours that is much faster than the increase in capacitance. This is likely due to surface conductivity in margin areas of NLEs that have delaminations between the dielectric layers.
3. Biased testing at room conditions.
   a. Degradation during first 1000 hours of testing at 100 V in all lots remained below 1%, but then increased substantially and by 2000 hours the loss of capacitance varied from 4 to 20% depending on lot of NLEs. The result is due to moisture sorption that at room environments (~50% RH) occurs with a characteristic time of ~ 1000 hours.
   b. A decrease of capacitance after 140 hours of testing at 125 V and 20 ºC for dry samples (2.7%) was substantially less than for samples that absorbed moisture at room environments (20%).
   c. Degradation processes continued during storage at room environments following voltage stress testing. The rate of degradation decreased during the storage, but the higher was the rate during electrical stress testing, the greater is the rate of degradation during storage. Most likely, corrosion processes initiated under electrical stress can continue in unbiased parts.
   d. Leakage currents in different lots of NLEs can differ up to two orders of magnitude. However, the level of currents during voltage stress testing is not correlated with the rate of capacitance degradation.
4. High temperature storage.
   a. Storage of NLEs at 125 ºC for 4000 hours resulted in relatively minor variations of AC characteristics: capacitance on average reduced by 2.3% and ESR increased by 45%.
   b. Leakage currents increased after HTS125 by more than an order of magnitude. The increase was reversible, and the initial level of currents was restored after 100 hours of operation at RC and rated voltage. The effect is likely due to the charge trapping on deep states in the dielectric.

5. Highly accelerated life test.
    a. HALT was carried out at temperatures from 85 ºC to 145 ºC and stress voltages from 1.25VR to 2VR typically for 1000 hours. All failures were due to parametric degradation, and no catastrophic failures were observed.
    b. Leakage currents were decreasing up to two orders of magnitude in the process of HALT. The effect might be due to self-healing and/or to building up of the barrier at the polymer/aluminum interface in the process of gradual trapping of electrons onto deep states in the dielectric.
6. Reliability acceleration factors.
    a. Times to parametric failures were determined as times when capacitance dropped to 90% of its initial value. Distributions of TTF were approximated with a general Weibull log-linear model. Temperature was assumed to accelerate failures according to Arrhenius, and voltage according to a power law.
    b. In all cases, the slope of the Weibull distributions exceeded one, thus indicating were-out failures of NLEs. The useful time of capacitors was calculated as a time when the probability of failure increases to 1 %, $F(TTF_i) = 1\%$.
    c. Accelerated testing at room conditions showed that times to failure for samples containing moisture accumulated after long-term (few months) storage at room environments can be more than 5 times lower than for dry samples.
    d. Assessments based on HALT resulted in a strong voltage dependence of TTF_c ($2.6 < n < 8.6$) and a relatively weak temperature dependence ($E_a < 0.5$ eV). Calculated useful life at 65 ºC and 0.6VR varies for different lots of NLEs from 9.6 to 5800 years.

VIII. Acknowledgment

The author is thankful to Chris Tiu, GSFC NEPP Task Monitor, for the review and discussions, and to Peter Majewicz, NEPP program manager, for support of this study. This work could not have been done without help from the GSFC PA Lab specialists. I am also grateful to Chris Barth and Luis Pinero (GRC), Angelo Yializis and Sean Katsarelis (PCA) for consultations and samples provided for this study.

IX. References

[1] A. Yializis, "A disruptive DC link capacitor technology for use in electric drive inverters," in *2nd Passive Components Networking Days, PCNS* Bucharest, Romania, 2019, September 10-13, pp. 36-43.

[2] A. Yializis, "High Energy Density Solid Stare Polymer Capacitors for Space Applications," in *4th Space Passive Component Days (SPCD), International Symposium*, ESA/ESTEC, Noordwijk, The Netherlands, 2022, 11-14 October 2022.

[3] T. Doytchinov, D. Tyler, S. Lukich*, et al.*, "Exxcelia new MML technology for film capacitors miniaturization," in *4th Space Passive Component Days (SPCD), International Symposium*, ESA/ESTEC, Noordwijk, The Netherlands, 2022, 11-14 October 2022.

[4] M. Makdessi, A. Sari, P. Venet*, et al.*, "Lifetime estimation of high-temperature high-voltage polymer film capacitor based on capacitance loss," *Microelectronics Reliability,* vol. 55, pp. 2012-2016, 2015/08/01/ 2015

[5] H. M. Umran, F. Wang and Y. He, "Ageing: Causes and Effects on the Reliability of Polypropylene Film Used for HVDC Capacitor," *IEEE Access,* vol. 8, pp. 40413-40430, 2020

[6] Hua Li, Tian Qiu, Zheng Li*, et al.*, "Capacitance Loss Evolution of Zn-Al Metallized Film Capacitors Under Atmospheric Corrosion," presented at the January 2022 IEEE Transactions on Dielectrics and Electrical Insulation PP(99):1-1, 2022.

[7] A. Teverovsky, "Insulation resistance and leakage currents in MLCCs with cracks," presented at the ESA 1st International Symposium 'Space Passive Component Days', Noordwijk, The Netherlands, 2013. https://escies.org/webdocument/showArticle?id=984&groupid=6

[8] A. Teverovsky, "Leakage currents and gas generation in advanced wet tantalum capacitors," NASA/GSFC, Greenbelt, MD 2015, https://nepp.nasa.gov/.../2015-562-Teverovsky-Final-Paper-NEPPweb-TN2...

[9] A. Yializis and Y. Ozaki, "POLYMER NANOLAMINATE CAPACITORS," *ResearchGate,* 2013 https://www.researchgate.net/publication/288598913_Solid_state_Polymer-Multi-Layer_PML_capacitors

[10] J. R. Laghari and A. N. Hammoud, "A brief survey of radiation effects on polymer dielectrics," *IEEE Transactions on Nuclear Science,* vol. 37, pp. 1076-1083, 1990

[11] Z. Wang, H. Li, F. Lin*, et al.*, "Degradation of Metallized Film Capacitors under Co-60γ Radiation," in *2021 IEEE 4th International Electrical and Energy Conference (CIEEC)*, 2021, 28-30 May 2021, pp. 1-4.

[12] L. F. Mafra Mendes Freitas Santos, F. Chen Abrego, K. Franklin Albertin Torres*, et al.*, "Inducing aluminum oxide growth at room temperature and atmospheric pressure through low dose gamma-ray irradiation," *Radiation Physics and Chemistry,* vol. 204, p. 110666, 2023/03/01/ 2023 https://www.sciencedirect.com/science/article/pii/S0969806X22007290
[13] T. Qiu, H. Li, Z. Li*, et al.*, "Capacitance loss characteristics of metallized film capacitors under atmospheric corrosion," in *2022 IEEE International Conference on High Voltage Engineering and Applications (ICHVE)*, 2022, 25-29 Sept. 2022, pp. 1-4.
[14] N. Valentine, M. H. Azarian and M. Pecht, "Metallized film capacitors used for EMI filtering: A reliability review," *Microelectronics Reliability,* vol. 92, pp. 123-135, 2019/01/01/ 2019 https://www.sciencedirect.com/science/article/pii/S0026271418310679
[15] T. Yunxiao, C. Pengqi, J. Yang*, et al.*, "Failure mechanism and life estimate of metallized film capacitor under high temperature and humidity," *Microelectronics and reliability,* vol. 137, 2022
[16] C. Lv, J. Liu, Y. Zhang*, et al.*, "Reliability Modeling for Metallized Film Capacitors Based on Time-Varying Stress Mission Profile and Aging of ESR," *IEEE Journal of Emerging and Selected Topics in Power Electronics,* vol. 9, pp. 4311-4319, 2021
[17] J. Dye, "Low Voltage PML Capacitor Development and Characterization," Sandia 2021, https://www.osti.gov/servlets/purl/1866907
[18] TDK, "Film Capacitor," in *General technical information*, 2018, https://www.tdk-electronics.tdk.com/download/530754/480aeb04c789e45ef5bb9681513474ba/pdf-generaltechnicalinformation.pdf.
[19] C. W. Reed and S. W. Cichanowskil, "The fundamentals of aging in HV polymer-film capacitors," *IEEE Transactions on Dielectrics and Electrical Insulation,* vol. 1, pp. 904-922, 1994
[20] J. Gorobez, B. Maack and N. Nilius, "Growth of Self-Passivating Oxide Layers on Aluminum—Pressure and Temperature Dependence," *physica status solidi (b),* vol. 258, pp. n/a-n/a, 2021
[21] A. Teverovsky, "Degradation of Aluminum and Tantalum Wet Electrolytic Capacitors during High Temperature Storage," in *4th PCNS Passive Components Networking Symposium*, Sønderborg, Denmark, 2023, September 11-13, pp. 129-140.
[22] AVX, "Polymer film," https://datasheets.kyocera-avx.com/AVX-FHC-Series.pdf.
[23] AVX, "FFVS, DC FILTERING, datasheet," https://datasheets.kyocera-avx.com/ffvs.pdf.
[24] CDE, "Power Film Capacitor Application Guide," https://www.cde.com/resources/technical-papers/filmAPPguide.pdf
[25] KEMET, "Polymer film capacitor," https://connect.kemet.com:7667/gateway/IntelliData-ComponentDocumentation/1.0/download/datasheet/C4AQLBU4560A1WK.pdf.
[26] Vishay, "General technical information. Film capacitors.," 2022 https://www.vishay.com/docs/26033/gentechinfofilm.pdf